Numerical Simulations of a Tropical Cyclone using the Arakawa-Schubert Scheme with Vertically Variable Entrainment Rate

Akihiko MURATA and Mitsuru UENO

Meteorological Research Institute / Japan Meteorological Agency, Tsukuba, Ibaraki 305-0052, Japan
(corresponding author: amurata@mri-jma.go.jp)

1. Introduction

Numerical simulations for tropical cyclones provide an extremely useful test for the depth of knowledge about cumulus parameterization (Ueno, 2000). We therefore have investigated effects of some cumulus parameterizations on tropical cyclone simulations. As a consequence it was found that the Arakawa-Schubert scheme guaranteed relatively good performance (e.g., Murata and Ueno, 2000). It has been pointed out, however, that fractional entrainment profiles in the scheme did not agree with those of observations and numerical experiments. Lin (1999) investigated entrainment profiles using simulated data from a slab-symmetric cloud-resolving model. He found that entrainment for each cloud type, which was categorized in terms of cloud top height, tended to be significant near cloud base and cloud top.

In this study, on the basis of the results from the three-dimensional cloud-resolving model (CRM), vertically variable entrainment rate is applied to a version of the Arakawa-Schubert scheme. The impact of the modified scheme on the simulations of typhoon Saomai (2000) is investigated.

2. Estimate of entrainment rate with a cloud-resolving model

The Meteorological Research Institute / Numerical Prediction Division nonhydrostatic model (MRI/NPD-NHM; Saito et al., 2001) with 200 m horizontal resolution is used as CRM. The model includes bulk cloud microphysics by Ikawa et al. (1991), which predicts the mixing ratios of six water species (water vapor, cloud water, rain, cloud ice, snow and graupel) and the number concentration of cloud ice. A domain (280×280) is set on a spiral rainband of Saomai. A 20-min simulation is conducted by using a one-way nest with output from the 1-km grid MRI/NPD-NHM.

Before the calculation of entrainment rate, a cumulus area, where a single cumulus is contained, is extracted from the CRM output. The calculation is conducted on the basis of the definition, dM/Mdz, where M is mass flux averaged over cumulus grids and z is height. The cumulus grids are defined as those at which the sum of mixing ratios as to cloud water and cloud ice is larger than 0.1 g/kg and vertical velocity is positive.

The result of the calculation clearly shows high entrainment rate just above the cloud base and just below the cloud top. Figure 1 displays the characteristic entrainment profiles that have larger amounts between 1.0 and 1.5 km high and between 6.5 and 7.0 km high. The layers in between are marked by relatively low entrainment rate.

3. Experimental design

MRI/NPD-NHM with 20-km horizontal grid length is used in the simulations of Saomai. We incorporate a version of the Arakawa-Schubert (AS) scheme (Kuma et. al. 1993), which has the prognostic equation that predicts the cloud base mass flux and has a downdraft and a mid-level convection, into MRI/NPD-NHM.

A profile of entrainment rate, λ, in the AS scheme is modified so that they can qualitatively represent the feature revealed in the CRM result. The assumed profile is as follows:

$$\lambda = A\{1-\sin(\frac{2\Delta}{z_T - z_B} z + \frac{\pi}{2} - \frac{z_T + z_B}{z_T - z_B}\Delta)\} + S$$

$$A > 0, S > 0, \Delta < \pi / 2$$

where z_B and z_T are cloud base and top height, respectively. Among unknown constants, Δ is set at 5×10^{-3}. The remaining constants A and S are determined so that following two conditions are satisfied. One of them is that the cloud top level is located where buoyancy in the cloud disappears. The other condition is that the entrainment rate at the cloud base, λ_B, is determined on the basis of the CRM result, which indicates that λ_B falls within the range between the order of 10^{-3} to 10^{-2} m^{-1}. As for the AS scheme, λ ranges from the order of 10^{-4} to 10^{-3} m^{-1}. λ_B therefore is set at $\lambda_B = k\lambda$, where k is constant that controls the degree of the cloud-base entrainment rate. With k varying among 2, 3, 5 and 10 (referred as the experiments of AS2, AS3, AS5 and AS10, respectively), 36-hr integrations are conducted to examine the sensitivity of k.

4. Results of numerical experiments

Difference in the entrainment rate profile has drastic influence on simulated precipitation patterns. The axisymmetric eyewall is reproduced in AS5, whereas more scattered feature is shown in AS (Fig.2). The precipitation in the former tends to lie in the location relatively near the storm center. The radial profiles of accumulated rainfall amount are shown in Fig.3. From the figure, it is found that the rainfall amount over the outer area (outside the 200 km radius) decreases with increases in the entrainment rate (i.e., increases in k).

The radial distribution of precipitation seems to play a role in the size of the simulated tropical cyclone. The radial profiles of the axisymmetric tangential wind velocity change (Fig.4) clearly shows that the quantities over the outer area decrease with increasing the cloud-base entrainment rate, which is the same aspect as the precipitation. The result indicates that the storm grows as the entrainment rate drops.

The less rainfall over the outer area in the larger entrainment case is accounted for by relatively little mass flux calculated by the modified scheme. The vertical profiles of the cloud mass flux, averaged over the area ranging from 200 to 500 km radii, display that the mass flux is weaker in the larger entrainment cases (Fig.5), suggesting that vertical static instability in the outer area is not eliminated so much as those of the smaller entrainment cases.

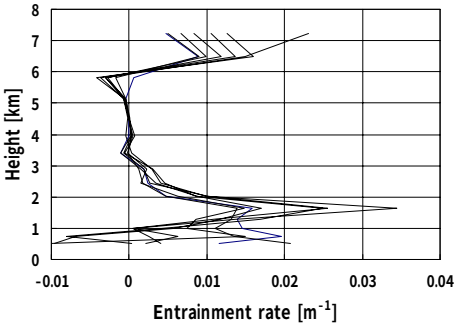

Fig.1 Vertical profiles of entrainment rate calculated by the CRM output. Lines are drawn every 5 sec from 6 min to 6 min 30 sec.

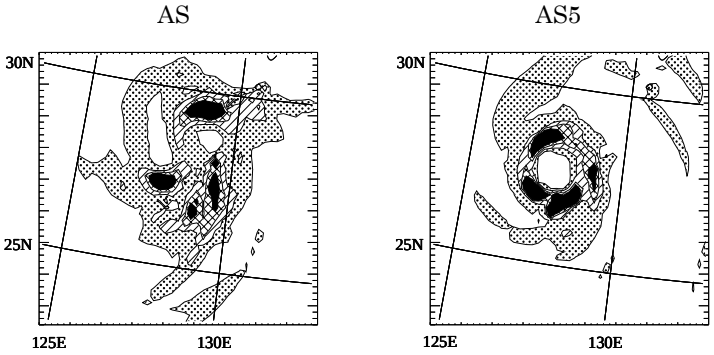

Fig.2 Horizontal distributions of 1-hr accumulated rainfall amount at 24 hr. Contours are drawn at 1, 5, 10 and 15 mm/hr.

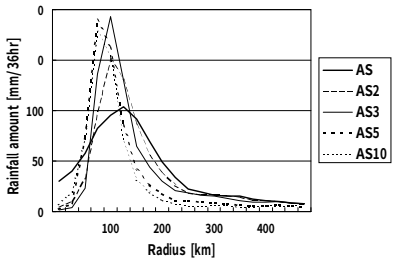

Fig.3 Radial profiles of azimuthally averaged 36-hr accumulated rainfall amount.

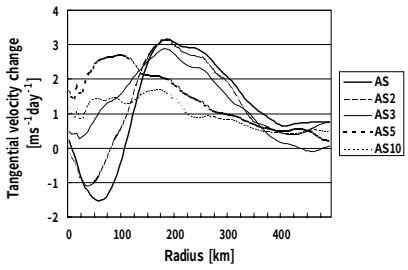

Fig.4 Radial profiles of azimuthally averaged tangential wind velocity change (between the initial and the end of the integration) on the surface. Unit is transformed to ms^{-1} day^{-1}.

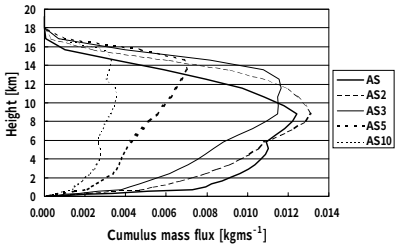

Fig.5 Vertical profiles of areally (200-500 km radii) and temporally (36 hr) averaged cumulus mass flux.

References

Ikawa, M., H. Mizuno, T. Matsuo, M. Murakami, Y. Yamada and K. Saito, 1991: Numerical modeling of the convective snow cloud over the Sea of Japan. -Precipitation mechanism and sensitivity to ice crystal nucleation rates-. J. Meteor. Soc. Japan, **69**, 641-667.

Kuma, K., C.-H. Cho, C. Muroi and M. Ueno, 1993: Improvement of typhoon track forecast by the JMA global model: An impact of cumulus parameterization. Papers presented at the third Technical Conference on SPECTRUM. Report No. TCP-33, WMO/TD-No. 595. World Meteor. Org., Geneva, Switzerland, Ⅳ 1-8.

Lin, C., 1999: Some bulk properties of cumulus ensembles by a cloud-resolving model. Part II: Entrainment profiles. J. Atmos. Sci., **56**, 3736-3748.

Murata, A. and M. Ueno, 2000: The Effects of different cumulus parameterization schemes on the intensity forecast of typhoon Flo (1990). J. Meteor. Soc. Japan, **78**, 819-833.

Saito, K., T. Kato, H. Eito and C. Muroi, 2001: Documentation of the Meteorological Research Institute / Numerical Prediction Division unified nonhydrostatic model. Tec. Rep. MRI, **42**, 133pp.

Ueno, M., 2000: Numerical prediction for tropical cyclones. Meteorology Research Note, **197**, 131-286 (in Japanese).